Gait & Posture 97 (2022) 28–34

Contents lists available at ScienceDirect

Gait & Posture

journal homepage: www.elsevier.com/locate/gaitpost

Accuracy of a 3D temporal scanning system for gait analysis: Comparative with a marker-based photogrammetry system

Ana V. Ruescas Nicolau [a,*], Helios De Rosario [a], Fermín Basso Della-Vedova [a], Eduardo Parrilla Bernabé [a], M.-Carmen Juan [b], Juan López-Pascual [a]

[a] Instituto de Biomecánica de Valencia, Universitat Politècnica de València, edifici 9C. Camí de Vera, s/n, 46022 València, Spain
[b] Instituto Universitario de Automática e Informática Industrial, Universitat Politècnica de València, edifici 1F. Camí de Vera, s/n, 46022 València, Spain

ARTICLE INFO

Keywords:
3D temporal scanner
Stereophotogrammetry
Markerless
Gait analysis
Landmark position error

ABSTRACT

Background: Combining the accuracy of marker-based stereophotogrammetry and the usability and comfort of markerless human movement analysis is a difficult challenge. 3D temporal scanners are a promising solution, since they provide moving meshes with thousands of vertices that can be used to analyze human movements.
Research question: Can a 3D temporal scanner be used as a markerless system for gait analysis with the same accuracy as traditional, marker-based stereophotogrammetry systems?
Methods: A comparative study was carried out using a 3D temporal scanner synchronized with a marker-based stereophotogrammetry system. Two gait cycles of twelve healthy adults were measured simultaneously, extracting the positions of key anatomical points from both systems, and using them to analyze the 3D kinematics of the pelvis, right hip and knee joints. Measurement differences of marker positions and joint angles were described by their root mean square. A t-test was performed to rule out instrumental errors, and an F-test to evaluate the amplifications of marker position errors in dynamic conditions.
Results: The differences in 3D landmark positions were between 1.9 and 2.4 mm in the reference pose. Marker position errors were significantly increased during motion in the medial-lateral and vertical directions. The angle relative errors were between 3% and 43% of the range of motion, with the greatest difference being observed in hip axial rotation.
Significance: The differences in the results obtained between the 3D temporal scanner and the marker-based system were smaller than the usual errors due to lack of accuracy in the manual positioning of markers on anatomical landmarks and to soft-tissue artefacts. That level of accuracy is greater than other markerless systems, and proves that such technology is a good alternative to traditional, marker-based motion capture.

1. Introduction

Over the last decades, human motion analysis has been widely used in research and for several applications in sports and medicine. Technology has continuously evolved to adapt to the growing demand for precise and accurate methods to capture human movement [1]. This demand is particularly relevant in the clinical setting, in which human motion analysis is used to support decision making. Specifically, 3D gait analysis already plays a role in the treatment of musculoskeletal and neurological pathologies [2,3]. Such information has proven to be useful in diagnostic thinking, treatment planning, and improving patient outcomes [4].

Marker-based stereophotogrammetry (MBSP) is currently the most accurate and widely used approach in biomechanical laboratories [5,6]. Joint angles are usually calculated as the relative rotation between proximal and distal local reference frames, which are defined by the direction of some axes and planes determined by anatomical landmarks, often associated to physical markers or calculated from them [7].

The instrumentation needed in maker-based approaches limits their utility in certain areas of sports biomechanics and rehabilitation, due to long participant preparation times, difficulties in attaching markers, and specially the physical and psychological constraints that the attachment of markers imparts on participants [5]. Several technologies have emerged over the years to overcome those limitations. Although inertial

* Corresponding author.
E-mail addresses: ana.ruescas@ibv.org (A.V. Ruescas Nicolau), helios.derosario@ibv.org (H. De Rosario), fermin.basso@ibv.org (F. Basso Della-Vedova), eduardo.parrilla@ibv.org (E. Parrilla Bernabé), mcarmen@dsic.upv.es (M.-C. Juan), juan.lopez@ibv.org (J. López-Pascual).

https://doi.org/10.1016/j.gaitpost.2022.07.001
Received 17 March 2022; Received in revised form 26 May 2022; Accepted 3 July 2022
Available online 5 July 2022
0966-6362/© 2022 The Authors. Published by Elsevier B.V. This is an open access article under the CC BY license (http://creativecommons.org/licenses/by/4.0/).

sensors (IMUs) have become very popular in biomechanics, they also have some disadvantages. IMUs, which are usually attached to the human body on elastic straps, are strongly affected by vibrations and soft tissue artefacts, and the misplacement of the sensors can lead to wrong measurements [1]. Video-based markerless motion capture is a potential alternative that improves usability. However, current commercial solutions like Microsoft Kinect, Kinovea or novel approaches as deep learning algorithm-based systems are still far from the performance provided by stereophotogrammetry [1,8], and the precision of markerless techniques is often regarded as too low for biomechanics analysis, especially for transverse plane rotations [5].

In the field of anthropometry, 3D temporal scanners (3DTS) have emerged to deal with applications that require capturing the human shape during motion, as clothing pattern design [9,10]. Such systems can provide sequences of meshes of thousands of points with less than 1 mm resolution at high speed [11,12]. The application of that technology to human movement analysis is still limited; however, some 3DTS provide trackable meshes with high precision and they are a promising alternative for markerless analysis of segmental and joint kinematics.

For a 3DTS-based system to be regarded as an adequate alternative to traditional motion capture, it should be at least capable to provide results comparable to those of a stereophotogrammetry-based system, when the same measurement protocols and analysis procedures are used. In such comparisons, discrepancies in the results are expected to depend on the errors of both systems in the identification of landmarks positions, and on the propagation of those errors to kinematic parameters. The study presented in this paper tests that assumption for lower limb kinematics during gait, tracking pelvic and leg motion simultaneously with MBSP and 3DTS.

2. Methods

2.1. Subjects

Twelve healthy adults (7 men, 5 women; age: 39.1 ± 9.8 years; height: 169.2 cm ± 9.1 cm; weight: 67.2 kg ± 14.9 kg; body mass index: 23.2 ± 3.7 kg/m^2) volunteered to participate in the study after providing informed written consent. The study was approved by the ethics committee of the Universitat Politècnica de València (P05_16_02_2022), and conduced in accordance with the declaration of Helsinki.

The sample size was calculated assuming that the resolution of the mesh (around 5 mm between vertices) caused a normally distributed random error, such that the mean of the differences between systems calculated for a sample of twelve subjects would have a standard error of 1.4 mm, which is smaller than the smallest intra-examiner error in the location of the anatomical landmarks that were used in the study, according to bibliography [13].

2.2. Materials

The experiment was conducted in the Human Analysis Laboratory of the Instituto de Biomecánica de Valencia. Two measurement systems were used in the experiment. A MSBP system (Kinescan/IBV) was used to capture the 3D location of markers attached to the body with 16 infrared cameras [14]. A 3DTS with 16 camera modules (Move4D/IBV) was used to register the 3D point cloud and color information of the whole body in motion [15]. Both systems were installed in a recording area of 3 x 2 m and 2.8 m high, and calibrated with a shared coordinate system before each measurement session, in order to relate the results to the same reference frame. Both systems were configured to record at 30 frames per second.

2.3. Measurement procedure

Subjects were instrumented with reflective markers on landmarks positions, manually identified by a physiotherapist (Fig. 1): the right/left superior anterior/posterior iliac spines (R_ASIS, L_ASIS, R_PSIS, L_PSIS), and the lateral epicondyle and malleolus (LE, LM) of the right leg. Two additional markers on the lateral aspect of the thigh (THI) and shank (SH) were used in order to analyze the rigid motion of those body segments. Planar adhesive markers instead of spherical markers were used to avoid interference in the 3DTS scanner reconstruction of the body shape. Knee and ankle widths were measured with a Vernier caliper for the definition of their joint centers, as explained below.

Each subject was recorded in a static measurement in standing posture and two gait measurements. In the static posture the subjects stood upright with legs separated at the level of the shoulders, and slightly abducted arms (around 30º). Gait measurements were performed in an 8 m corridor. Participants were instructed to walk straight at comfortable speed, and a warmup of several trials was performed before recording, to familiarize the subject with the procedure. The gait captures were made after the subjects had started walking.

2.4. Data processing

2.4.1. Tracking of marker positions

The positions of the 8 reflective markers were tracked by the MBSP system, and their trajectories were assigned to each marker by manual identification of the first frame.

The 3DTS produced a series of watertight homologous meshes with 49,530 vertices distributed at 5 mm average distance from each other that could be tracked across frames [16,17]. The vertices of the meshes corresponding to the markers were defined in the reference posture, by manual identification of the nearest vertex to the center of the marker in textured OBJ files (Fig. 1). The identification was made individually for every subject, by a single operator. Then, the 3D trajectories of those vertices were automatically extracted for the gait measurements.

2.4.2. Kinematic analysis

The position of joint centers was defined in the reference posture as follows. The hip joint center (HJC) was calculated using Harrington's method [18], using the position of pelvic markers and estimating leg length as the distance between R_ASIS and LM. The knee joint center (KJC) was obtained through a "chord function", using the measured knee width and a variation of the reference points described by the Plug-In Gait Guide [19]. The frontal plane containing the KJC in the reference posture was defined as passing through HJC and LE, and parallel to the R_ASIS-L_ASIS line. The same method was used to obtain the ankle joint center (AJC), using KJC, LM and the R_ASIS-L_ASIS line to define the plane that contains the joint, and the measured ankle width.

The joint reference frames of hip, knee and ankle, as well as the order and direction of their relative rotations, were defined following the ISB recommendations [20,21]. During the measurements, the positions and orientations of joint centers and reference frames were recalculated using rigid body transformations: HJC and KJC trajectories were calculated as belonging to the pelvis and the thigh, respectively; the motion of the pelvis was determined by the trajectories of pelvic markers, the thigh by THI, LE and HJC, and the shank by SH, LM and KJC.

Hip and knee joint rotations were calculated as *ZXY* Euler sequences, obtaining the angles of flexion-extension (FE), lateral flexion (LF) and axial rotation (AR) through one stride of each subject. Pelvic tilt (T), obliquity (O) and rotation (R) were calculated as recommended in [22]. All the calculations were done independently for landmark positions obtained by photogrammetry and identified on the 3D mesh.

2.4.3. Statistical analysis

The positions of markers and all joint angles were extracted to compare the results of the MBSP and 3DTS systems. Hip and knee FE curves were used to mark one gait cycle in each measurement manually, and to adjust delays by maximization of cross-correlations between the

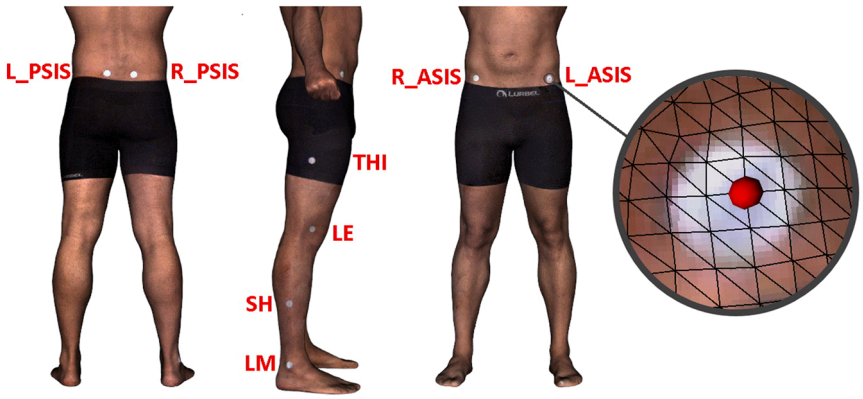

Fig. 1. Planar reflective markers location on a 3D textured mesh and selection of the closest vertex to the center of the L_ASIS marker.

curves. Accidental errors due to partial marker occlusion or reconstruction of the mesh were detected as outliers in the curves (spurious peaks that differed from the surrounding values more than the range of the variable excluding those points), and those data points were removed from the measurements in both instruments.

The differences between the results obtained by either system were used as measures of error. The errors of marker coordinates were described by their mean and standard deviation in each axis of the coordinate system, for the reference posture and all measurements of every subject.

For the reference posture, a grand mean and standard deviation was also calculated as a measure of instrumental error, and a t-test was performed across subjects to verify that there was no deviation due to the misalignment of the calibrated reference frames. The overall root mean square (RMS) of marker position errors in the reference posture was also calculated to quantify the size of the error under the assumption of zero mean, and this was compared to the same value calculated in dynamic conditions (gait cycles). F-tests were used to assess the amplification of the error in motion, assuming that the squares of the RMS were distributed as Chi-squared values (squares of random normal variables with zero mean).

Joint angle curves were adjusted to a common time scale between 0% and 100% of the gait cycle by linear interpolation to facilitate a visual comparison of different measurements. The differences between systems described by the RMS of each measurement, as well as by the differences in ROM, were compared though Bland-Altman plots.

All calculations were made in Julia and Python.

3. Results

Two gait cycles from each subject were analyzed, yielding a total of 24 gait cycles. 7 frames with outliers were detected and removed from the data sequence of 2 measurements.

Table 1 shows the size of instrumental errors and the statistical tests performed on them. The results of the tests show that the errors could be regarded as having zero mean ($p > 0.05$), i.e. there was no significant deviation between the calibration frames of both measurement systems.

Table 2 shows the size of measurement errors in marker coordinates,

Table 1
Summary of differences between anatomical marker coordinates (MBSP - 3DTS) in the reference posture, and t-test contrasting the hypothesis of null mean. AP: Anterior-Posterior direction; ML: Medial-lateral direction; VT: Vertical direction.

	Mean and std. dev of error (mm)	t-test
AP	-0.86 (2.26)	$T(11) = -2.101$, $p = 0.060$
ML	-0.04 (1.90)	$T(11) = -0.147$, $p = 0.886$
VT	-0.15 (2.14)	$T(11) = -0.520$, $p = 0.613$

Table 2
RMS of differences in marker coordinates in static (reference posture) and dynamic (gait) conditions, and F-test contrasting the hypothesis of equal amplitudes. AP: Anterior-Posterior direction; ML: Medial-lateral direction; VT: Vertical direction.

	Static (mm)	Dynamic (mm)	F-test
AP	2.40	3.91	$F(23,11) = 2.652$, $p = 0.096$
ML	1.89	3.74	$F(23,11) = 3.923$, $p = 0.022$
VT	2.14	4.80	$F(23,11) = 5.016$, $p = 0.008$

comparing the results in static and dynamic conditions. It was observed that the differences in marker coordinates in motion were between 1.6 and 2.2 times greater than in static conditions, and that amplification was statistically significant in the medial-lateral and vertical directions ($p < 0.05$).

Fig. 2 shows the temporal distributions of hip, knee and pelvic angles through the gait cycle, for both measurement systems. The differences between systems are quantified in Table 3. The differences in pelvic angles and in joint FE angles were the smallest, with maximum values below 3°. The greatest errors were found in hip AR, with mean RMS 5.8°, 43.3 % of range of motion (ROM), followed by knee LF (mean RMS 3.5°, 37.1 % of ROM) and AR (mean RMS 3.6°, 14.8 % of ROM).

Those RMS values are correlated with the dispersion of differences in ROM, which are represented in the Bland-Altman plots (Fig. 3). Those plots also show that the ROM measured by 3DTS was systematically greater for knee FE and pelvis R, but smaller for hip LF and pelvis O, when compared with MBSP measurements; those differences were in the majority of cases smaller than 5°.

4. Discussion

This study assessed the accuracy of a 3DTS for human gait analysis, compared with MBSP. Having high-density meshes of points that represent the full surface of the subject's skin, without any need of instrumentation, is a potential big advantage, which enables to conduct advanced analyses considering not only changes in position, but also in shape. However, in order to trust that technology, it is necessary to prove that the shape and deformation of the mesh of points follows the anatomy of the subjects. This hypothesis was tested for 8 points of the pelvis and lower limb that are routinely used in gait analysis, considering their 3D coordinates and their effect on hip and knee angles.

The differences in landmark 3D locations were between 1.9 and 2.4 mm in static posture, due to the finite resolution of the homologous mesh and to possible imprecisions of the calibration of both systems. During gait, the positions of those points in the mesh departed up to nearly 5 mm in the vertical direction, and less than 4 mm in the horizontal plane, from the centers of the markers observed by

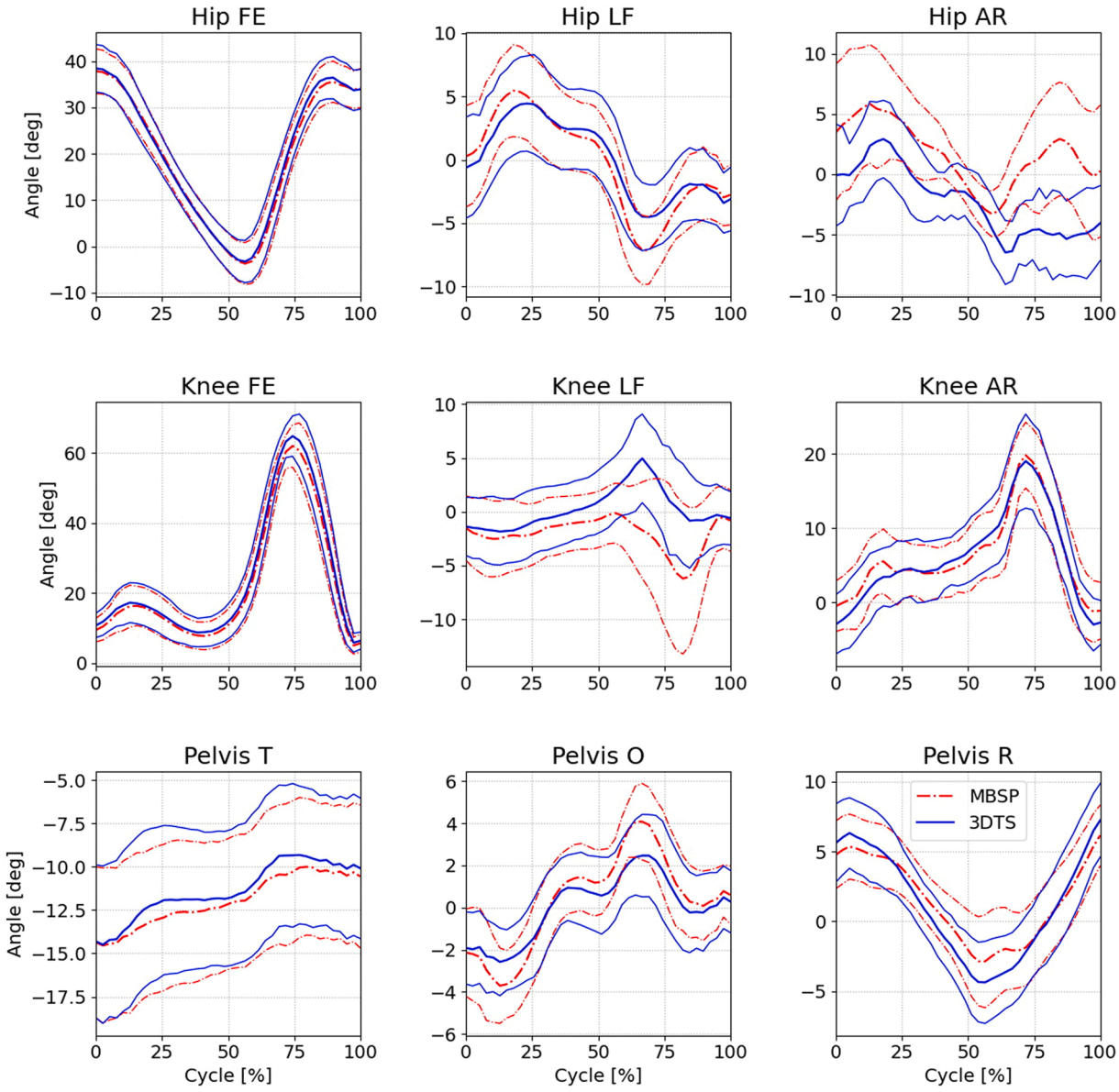

Fig. 2. Hip, knee and pelvic angles: Mean curves (thick lines) of the 24 samples for the MBSP (red-dotted) and 3DTS (blue-solid), during one gait cycle. Thin upper and lower lines are the mean ± the standard deviation of the adjusted curves at each point.

Table 3
Summary of the joint angle errors (RMS of differences between MBSP and 3DTS, calculated for each measurement): mean, standard deviation (SD) and maximum of RMS, and relative size of mean RMS with respect to mean range of motion (ROM). FE, flexion-extension; LF, lateral flexion; AR, axial rotation; T, tilt; O, obliquity, R, rotation. Absolute values in degrees.

	Hip			Knee			Pelvis		
	FE	LF	AR	FE	LF	AR	T	O	R
Mean RMS	1.26	1.65	5.76	1.98	3.51	3.62	0.90	1.15	1.19
SD RMS	0.30	0.44	1.95	0.37	1.23	1.34	0.45	0.35	0.42
Max RMS	1.88	2.59	9.09	2.88	6.51	5.90	1.95	1.76	1.96
Mean ROM	42.87	11.96	13.28	60.53	9.47	24.47	5.80	7.37	11.62
% mean RMS	3.0 %	13.8 %	43.3 %	3.3 %	37.1 %	14.8 %	15.5 %	15.5 %	10.2 %

stereophotogrammetry. Since STA and other instrumental errors affect the measurements of both systems, it was not possible to conduct a precise assessment of the landmark location error associated specifically to the 3DTS. But the comparison of such differences with the usual size of those types of errors can be used to gauge the impact of changing the technology.

In all cases the differences between instruments were smaller than usual instrumental and procedural errors. The uncertainty in the location of anatomical landmarks of the lower limb varies across body parts, with an intra-examiner error of 6.7 mm for LM, 10 mm for LE, and between 11.5 and 21 mm for pelvic markers — which increases by a factor of two for most landmarks when different examiners are involved [13].

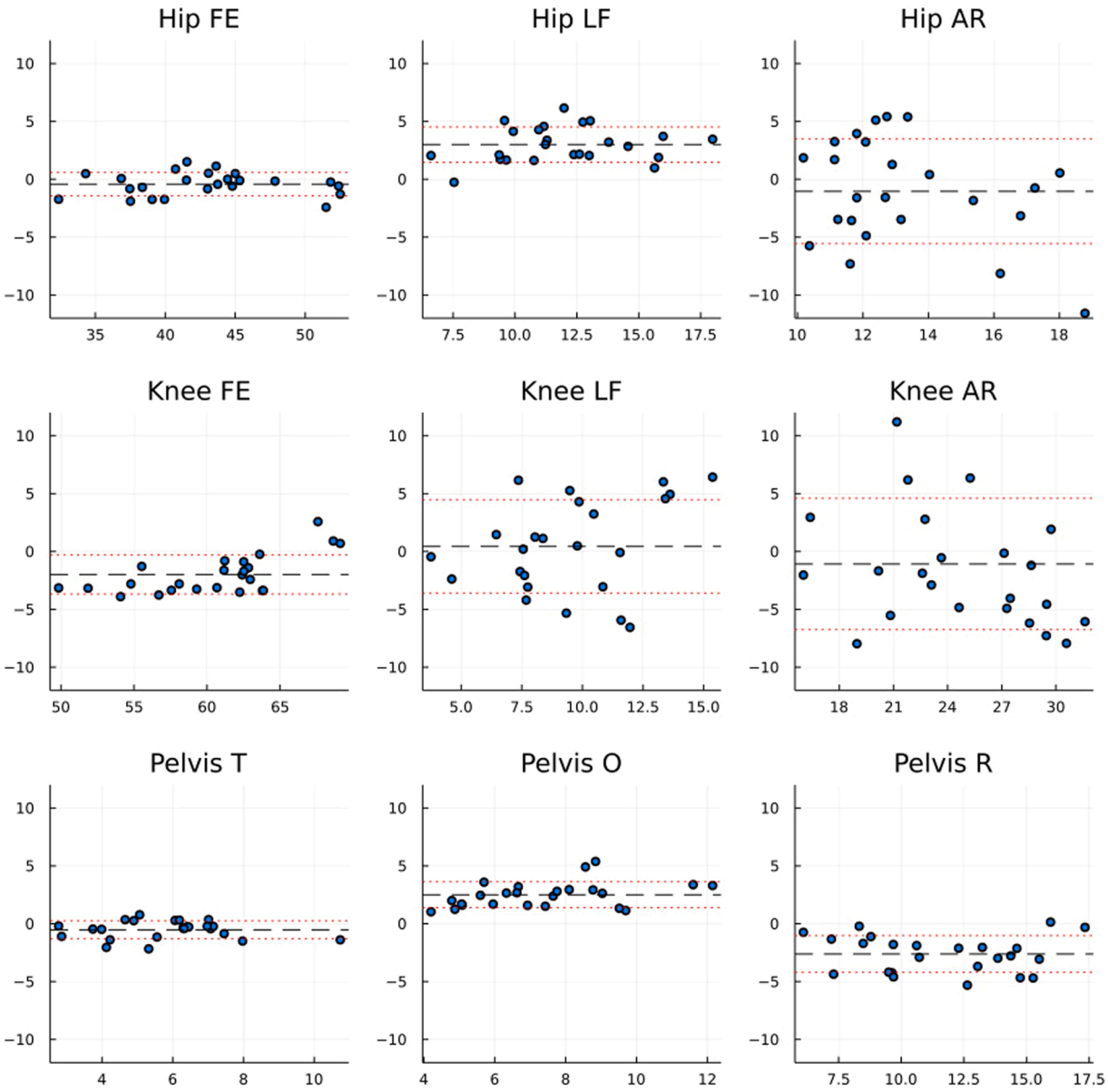

Fig. 3. Bland-Altman plots of ROM differences between measurements analyzed by MBSP and 3DTS. Average ROM in the X-axis, and difference in ROM between systems in the Y-axis. Positive values mean greater ROM measured by MBSP. FE, flexion-extension; LF, lateral flexion; AR, axial rotation; T, tilt; O, obliquity, R, rotation. Absolute values in degrees.

In the presence of STA, marker position errors relative to anatomical landmarks reported by different studies increase with a median from 2.4 to 8.2 mm in the shank, 7.6–13.7 mm in the thigh, and 3.1–52.1 mm in the pelvis [23,24].

Joint angle errors were of the same order of magnitude for hip and knee. The average RMS of the difference between both systems was between 1.3° and 5.8° degrees, with a maximum of 9.1° degrees. That was similar to the uncertainty in joint rotations usually introduced by intra-examiner marker positioning errors. AR, which is the angle that is usually more prone to errors, showed the greatest differences, slightly greater than inter-examiner errors for the hip (5.6°), and smaller than inter-examiner errors for the knee (10°) [13]. The added impact of STA on lower limb kinematics is greater: knee rotation errors vary between 1.4° and 15° [25]. In-vivo quantifications of hip kinematic errors is more difficult to find due to safety implications of measuring the pelvic region with fluoroscopy or other invasive techniques [26]; considering the results of the study conducted by Fiorentino et al. [27], and assuming that they represent the distribution of random normal variables, the equivalent RMS of their reported errors (FE 1.9°, LF 0.67°, AR 6.3°) were similar to the ones obtained in this study.

The approach used in this study, based on tracking fixed points of the mesh obtained by a 3DTS, produced results that were more consistent with MBSP measurements than other markerless approaches, like the segmentation of visual hulls [28] or the automatic detection of salient points in images [8], which yielded errors in marker positions and joint angles one order of magnitude greater. Therefore, 3DTS can be regarded as the markerless technology which provides joint angles that are closer to those obtained with an MBSP when equivalent protocol and data processing are used.

Tracking a small set of landmarks as in conventional MBSP studies is, however, a very narrow exploitation of the information contained in 3DTS measurements. The homologous mesh allows to expand the set of available points for conventional analysis techniques to an extent that is unwieldly with physical markers, which is an advantage e.g. to conduct analyses of STA [29,30]. It is also possible to analyze the shape of body segments, to estimate body segment inertial parameters [31], and

exploit other topological data. The benefit of those advantages, besides the fact of not having to instrument the users, can compensate current drawbacks of 3DTS technology, such as the higher cost of equipment and having to manage larger data sets, or limitations in the kind of scenes that can be tracked; e.g. the equipment used in this study can only track a single person at a time, who does not wield implements or interacts with objects of the surrounding environment. Also, the system works with a single mesh template, which is designed to fit a typical human body, and it does not work properly for subjects with unusual morphological traits like amputees.

This study is limited to the analysis of lower limb kinematics in healthy young adults, during level gait. In order to avoid distortions of the mesh due to the instrumentation, the spherical markers that are routinely used in MBSP were replaced by planar markers, which have worse visibility by cameras with oblique angle of vision with respect to their surface. This hindered the measurement of markers on the foot, which could not be placed in such a manner that they had the proper orientation for a sufficient number of cameras during the whole gait cycle, so that only hip and knee joints could be compared.

The mesh captured by the 3DTS has a fixed topology that allows to assign specific vertices to landmarks positions, ruling out the need of any kind of markers. This could be done by analyzing the distribution of closest vertices to the coordinates of the landmarks, in a larger database of scans where those landmarks have been annotated. A preliminary test of that approach is explored and shown in the supplementary material, using data from the CESAR database [32], to analyze the kinematics of the hip, knee and ankle of both sides.

It remains to be studied to what extent these results are valid with other profiles of subjects, parts of the body, and other gestures. Activities with greater ranges of motion or sudden movements may be more challenging due to greater STA, as well as gestures which imply close contact between body parts, since the collision between parts of the mesh (e.g. legs or arms) may produce greater deformations of its geometry.

Finally, the results presented in this manuscript are limited to the study of the movement of 8 vertices of the 3DTS mesh. Future experiments should be conducted to explore the potential use of the whole mesh for human motion analysis.

CRediT authorship contribution statement

Ana V. Ruescas Nicolau: Conceptualization, Data curation, Formal analysis, Investigation, Methodology, Project administration, Resources, Software, Supervision, Validation, Visualization, Writing – original draft, Writing – review & editing. **Helios De Rosario:** Conceptualization, Data curation, Formal analysis, Funding acquisition, Investigation, Methodology, Project administration, Software, Supervision, Validation, Visualization, Writing - original draft, Writing – review & editing. **Fermín Basso Della-Vedova:** Data curation, Formal analysis, Software, Validation, Visualization, Writing – review & editing. **Eduardo Parrilla Bernabé:** Conceptualization, Data curation, Software, Supervision, Validation, Writing – review & editing. **María Carmen Juan Lizandra:** Conceptualization, Methodology, Supervision, Validation, Writing – review & editing. **Juan López-Pascual:** Conceptualization, Formal analysis, Funding acquisition, Investigation, Methodology, Project administration, Supervision, Validation, Writing – original draft, Writing – review & editing.

Declaration of interest

None.

Acknowledgements

Activity developed within the framework of the IBERUS project. Technological Network of Biomedical Engineering applied to degenerative pathologies of the neuromusculoskeletal system in clinical and outpatient settings (CER-20211003), CERVERA Network financed by the Ministry of Science and Innovation through the Center for Industrial Technological Development (CDTI), charged to the General State Budgets 2021 and the Recovery, Transformation and Resilience Plan.

Appendix A. Supporting information

Supplementary data associated with this article can be found in the online version at doi:10.1016/j.gaitpost.2022.07.001.

References

[1] F. Roggio, S. Ravalli, G. Maugeri, A. Bianco, A. Palma, M.D. Rosa, G. Musumeci, Technological advancements in the analysis of human motion and posture management through digital devices, World J. Orthop. 12 (2021) 467–484, https://doi.org/10.5312/wjo.v12.i7.467.

[2] J.M. Motherwell, B.D. Hendershot, S.M. Goldman, C.L. Dearth, Gait biomechanics: a clinically relevant outcome measure for preclinical research of musculoskeletal trauma, J. Orthop. Res. 39 (2021) 1139–1151, https://doi.org/10.1002/jor.24990.

[3] R.A. States, J.J. Krzak, Y. Salem, E.M. Godwin, A.W. Bodkin, M.L. McMulkin, Instrumented gait analysis for management of gait disorders in children with cerebral palsy: a scoping review, Gait Posture 90 (2021) 1–8, https://doi.org/10.1016/j.gaitpost.2021.07.009.

[4] T.A.L. Wren, N.Y. Otsuka, R.E. Bowen, A.A. Scaduto, L.S. Chan, M. Sheng, R. Hara, R.M. Kay, Influence of gait analysis on decision-making for lower extremity orthopaedic surgery: Baseline data from a randomized controlled trial, Gait Posture 34 (2011) 364–369, https://doi.org/10.1016/j.gaitpost.2011.06.002.

[5] S.L. Colyer, M. Evans, D.P. Cosker, A.I.T. Salo, A review of the evolution of vision-based motion analysis and the integration of advanced computer vision methods towards developing a markerless system, Sport. Med. Open 4 (2018), https://doi.org/10.1186/s40798-018-0139-y.

[6] E. van der Kruk, M.M. Reijne, Accuracy of human motion capture systems for sport applications; state-of-the-art review, Eur. J. Sport Sci. 18 (2018) 806–819, https://doi.org/10.1080/17461391.2018.1463397.

[7] A. Cappozzo, U. Della Croce, A. Leardini, L. Chiari, Human movement analysis using stereophotogrammetry: Part 1: theoretical background, Gait Posture 21 (2005) 186–196, https://doi.org/10.1016/j.gaitpost.2004.01.010.

[8] R.M. Kanko, E.K. Laende, E.M. Davis, W.S. Selbie, K.J. Deluzio, Concurrent assessment of gait kinematics using marker-based and markerless motion capture, J. Biomech. 127 (2021), 110665, https://doi.org/10.1016/j.jbiomech.2021.110665.

[9] L. Benton, J.-C. Nebel, Study of the breathing pattern based on 4D data collected by a dynamic 3D body scanner, in: Paris, France, 2002. ⟨https://eprints.kingston.ac.uk/id/eprint/41986/⟩ (accessed January 25, 2022).

[10] Y.J. Wang, P.Y. Mok, Y. Li, Y.L. Kwok, Body measurements of Chinese males in dynamic postures and application, Appl. Ergon. 42 (2011) 900–912, https://doi.org/10.1016/j.apergo.2011.02.006.

[11] X. Huang, Y. Zhang, Z. Xiong, High-speed structured light based 3D scanning using an event camera, Opt. Express 29 (2021) 35864–35876, https://doi.org/10.1364/OE.437944.

[12] H.-T. Lübbers, L. Medinger, A. Kruse, K.W. Grätz, F. Matthews, Precision and accuracy of the 3dMD photogrammetric system in craniomaxillofacial application, J. Craniofacial Surg. 21 (2010) 763–767, https://doi.org/10.1097/SCS.0b013e3181d841f7.

[13] U. Della Croce, A. Cappozzo, D.C. Kerrigan, Pelvis and lower limb anatomical landmark calibration precision and its propagation to bone geometry and joint angles, Med. Biol. Eng. Comput. 37 (1999) 155–161, https://doi.org/10.1007/BF02513282.

[14] A. Page, P. Candelas, F. Belmar, Application of video photogrammetry to analyse mechanical systems in the undergraduate physics laboratory, Eur. J. Phys. 27 (2006) 647–655, https://doi.org/10.1088/0143-0807/27/3/017.

[15] E. Parrilla, A.-V. Ruescas, J.-A. Solves, A. Ballester, B. Nacher, S. Alemany, D. Garrido, A methodology to create 3D body models in motion, in: D.N. Cassenti, S. Scataglini, S.L. Rajulu, J.L. Wright (Eds.), Advances in Simulation and Digital Human Modeling, Springer International Publishing, Cham, 2021, pp. 309–314, https://doi.org/10.1007/978-3-030-51064-0_39.

[16] A. Ballester, A. Pierola, E. Parrilla, J. Uriel, A.V. Ruescas, C. Perez, J.V. Dura, S. Alemany, 3D Human Models from 1D, 2D and 3D Inputs: Reliability and Compatibility of Body Measurements, in: Proceedings of 3DBODY.TECH 2018 - 9th International Conference and Exhibition on 3D Body Scanning and Processing Technologies, Lugano, Switzerland, 16–17 Oct. 2018, Hometrica Consulting - Dr. Nicola D'Apuzzo, Lugano, Switzerland, 2018: pp. 132–141. ⟨https://doi.org/10.15221/18.132⟩.

[17] E. Parrilla, A. Ballester, P. Parra, A. Ruescas, J. Uriel, D. Garrido, S. Alemany, MOVE 4D: Accurate High-Speed 3D Body Models in Motion, in: Proc. of 3DBODY.TECH 2019, Lugano, Switzerland, 22–23 Oct. 2019, 2019: pp. 30–32. https://doi.org/doi:10.15221/19.030.

[18] M.E. Harrington, A.B. Zavatsky, S.E.M. Lawson, Z. Yuan, T.N. Theologis, Prediction of the hip joint centre in adults, children, and patients with cerebral palsy based on

magnetic resonance imaging, J. Biomech. 40 (2007) 595–602, https://doi.org/10.1016/j.jbiomech.2006.02.003.
[19] Plug-in Gait Reference Guide, (2021). ⟨https://docs.vicon.com/download/attachments/124850166/Plug-in%20Gait%20Reference%20Guide.pdf?version=1&modificationDate=1617008938000&api=v2⟩ (accessed November 4, 2021).
[20] E.S. Grood, W.J. Suntay, A joint coordinate system for the clinical description of three-dimensional motions: application to the knee, J. Biomech. Eng. 105 (1983) 136–144.
[21] G. Wu, S. Siegler, P. Allard, C. Kirtley, A. Leardini, D. Rosenbaum, M. Whittle, D. D. D'Lima, L. Cristofolini, H. Witte, O. Schmid, I. Stokes, ISB recommendation on definitions of joint coordinate system of various joints for the reporting of human joint motion—part I: ankle, hip, and spine, J. Biomech. 35 (2002) 543–548, https://doi.org/10.1016/S0021-9290(01)00222-6.
[22] R. Baker, Pelvic angles: a mathematically rigorous definition which is consistent with a conventional clinical understanding of the terms, Gait Posture 13 (2001) 1–6, https://doi.org/10.1016/S0966-6362(00)00083-7.
[23] V. Camomilla, T. Bonci, A. Cappozzo, Soft tissue displacement over pelvic anatomical landmarks during 3-D hip movements, J. Biomech. 62 (2017) 14–20, https://doi.org/10.1016/j.jbiomech.2017.01.013.
[24] A. Cereatti, T. Bonci, M. Akbarshahi, K. Aminian, A. Barré, M. Begon, D.L. Benoit, C. Charbonnier, F. Dal Maso, S. Fantozzi, C.-C. Lin, T.-W. Lu, M.G. Pandy, R. Stagni, A.J. van den Bogert, V. Camomilla, Standardization proposal of soft tissue artefact description for data sharing in human motion measurements, J. Biomech. 62 (2017) 5–13, https://doi.org/10.1016/j.jbiomech.2017.02.004.
[25] A. Peters, B. Galna, M. Sangeux, M. Morris, R. Baker, Quantification of soft tissue artifact in lower limb human motion analysis: a systematic review, Gait Posture 31 (2010) 1–8, https://doi.org/10.1016/j.gaitpost.2009.09.004.
[26] F. D'Isidoro, P. Eschle, T. Zumbrunn, C. Sommer, S. Scheidegger, S.J. Ferguson, Determining 3D kinematics of the hip using video fluoroscopy: guidelines for balancing radiation dose and registration accuracy, J. Arthroplast. 32 (2017) 3213–3218, https://doi.org/10.1016/j.arth.2017.05.036.
[27] N.M. Fiorentino, P.R. Atkins, M.J. Kutschke, J.M. Goebel, K.B. Foreman, A. E. Anderson, Soft tissue artifact causes significant errors in the calculation of joint angles and range of motion at the hip, Gait Posture 55 (2017) 184–190, https://doi.org/10.1016/j.gaitpost.2017.03.033.
[28] E. Ceseracciu, Z. Sawacha, C. Cobelli, Comparison of markerless and marker-based motion capture technologies through simultaneous data collection during gait: proof of concept, PLoS One 9 (2014), https://doi.org/10.1371/journal.pone.0087640.
[29] A. Ancillao, E. Aertbeliën, J. De Schutter, Effect of the soft tissue artifact on marker measurements and on the calculation of the helical axis of the knee during a gait cycle: a study on the CAMS-Knee data set, Hum. Mov. Sci. 80 (2021), 102866, https://doi.org/10.1016/j.humov.2021.102866.
[30] A. Barré, R. Aissaoui, K. Aminian, R. Dumas, Assessment of the lower limb soft tissue artefact at marker-cluster level with a high-density marker set during walking, J. Biomech. 62 (2017) 21–26, https://doi.org/10.1016/j.jbiomech.2017.04.036.
[31] T. Robert, P. Leborgne, G. Beurier, R. Dumas, Estimation of body segment inertia parameters from 3D body scanner images: a semi-automatic method dedicated to human movement analysis applications, Comput. Methods Biomech. Biomed. Eng. 20 (2017) 177–178, https://doi.org/10.1080/10255842.2017.1382920.
[32] S. Blackwell, K.M. Robinette, M. Boehmer, S. Fleming, S. Kelly, T. Brill, D. Hoeferlin, D. Burnsides, Civilian American and European Surface Anthropometry Resource (CAESAR). Volume 2: Descriptions, SYTRONICS INC DAYTON OH, 2002. ⟨https://apps.dtic.mil/sti/citations/ADA408374⟩ (accessed January 27, 2022).